



Prediction of failure in atmospheric ice under triaxial compressive stress



H. Farid *, A. Saeidi, M. Farzaneh

Canada Research Chair on Atmospheric Icing Engineering of Power Networks (INGIVRE) www.cigele.ca, University of Quebec in Chicoutimi, QC, Canada

ARTICLE INFO

Article history:

Received 12 July 2016

Received in revised form 3 January 2017

Accepted 7 March 2017

Available online 11 March 2017

Keywords:

Atmospheric ice

Triaxial load

Failure criteria

ABSTRACT

Triaxial experiments have been carried out on atmospheric ice samples under various conditions. Samples have been obtained from ice accumulated on a rotating cylinder inside the INGIVRE (Canada Research Chair on Atmospheric Icing Engineering of Power Networks) icing wind tunnel. Samples were tested at the same temperature at which they had been accumulated: at -5 , -10 and -15 °C under three strain rates 10^{-4} , 10^{-3} and 10^{-2} s^{-1} . Tests were conducted under various confinement pressures. At a temperature close to the melting point, atmospheric ice strength increases up to a certain value of confinement, and then decreases significantly. In the case where atmospheric ice strength increases continuously with increasing confinement for lower temperatures, the Mohr-Coulomb and Hoek-Brown failure criteria have been investigated in order to predict the failure of atmospheric ice.

© 2017 Elsevier B.V. All rights reserved.

1. Introduction

Failure of atmospheric ice is usually associated with a state of uniaxial stress. However, this approach is less accurate in presenting the associated phenomena with the failure of this type of ice. The literature includes a variety of works on uniaxial behavior of ice (Gold, 1977; Schulson, 1990; Arakawa and Maeno, 1997; Kermani et al., 2007), while little attention was paid to the states of more complex stresses. It is known that fracture of atmospheric ice is initiated by a complex stress field (Kermani, 2007).

Multiaxial tests, where the three main stresses vary independently of one another, have been carried out on ice (Schulson, 2001, 2006). However, triaxial testing, where uniaxial and hydrostatic pressure stresses are imposed, proved to be more practical to establish a uniform stress field for small sample sizes (Jones, 1982; Rist and Murrell, 1994).

Brittle failure of ice depends highly on hydrostatic pressure (Jones, 1982). At relatively high strain rates, Jones (1978) has observed during his triaxial tests on laboratory prepared ice, that the yield stress for polycrystalline ice increases initially with increasing confining pressure of up to 30 MPa. For higher confining pressures, yield stress decreases with further increase in hydrostatic pressure. The initial increase is thought to be due to the elimination of cracking and brittle failure by the confining pressure, thereby allowing the ice to deform plastically. Gagnon and Gammon (1995a), who have conducted triaxial experiments on iceberg and glacier ice, observed that ice strength increases with increasing hydrostatic pressure at low temperatures, while it

increases up to a certain level, and then decreases for temperatures close to the melting point.

Study of the behavior of atmospheric ice in triaxial state of stress needs a systematic experimental investigation of its brittle failure under combined stress. However, to the best of our knowledge, the literature contains no study of triaxial behavior of atmospheric ice. Other than studying the effect of hydrostatic pressure on the behavior of ice, triaxial tests aim to present a physical failure criterion, in which different structural and environmental parameters are taken into consideration, in order to provide a failure envelope that predicts the state of the stresses.

This study reports the effect of confining pressure on the mechanical parameters of atmospheric ice, under various loading conditions. Obtained experimental results will be used to identify the parameters in the Mohr-Coulomb and Hoek-Brown failure criteria for atmospheric ice.

2. Specimen preparation and test procedure

Atmospheric ice was prepared under specific conditions created in the atmospheric icing research wind tunnel at CIGELE (Canada Research Chair on Atmospheric Icing Engineering of Power Networks) Laboratories. This technique was used to simulate the natural atmospheric icing process, details about ice preparation procedure are explained elsewhere (Farid et al., 2016). More details on grains size, pores size and their distribution have been presented in the same reference, in the interests of clarity, a summary of these results has been also presented in Appendix B. Three accumulation temperatures were considered; -15 , -10 and -5 °C. Atmospheric ice was accumulated on a rotating aluminum cylinder (78-mm diameter and 590-mm length) as shown in Fig. 1(a). For all experiments, mean volume droplet diameter (MVD) was fixed at 40 μ m

* Corresponding author.

E-mail address: hicham.farid1@uqac.ca (H. Farid).

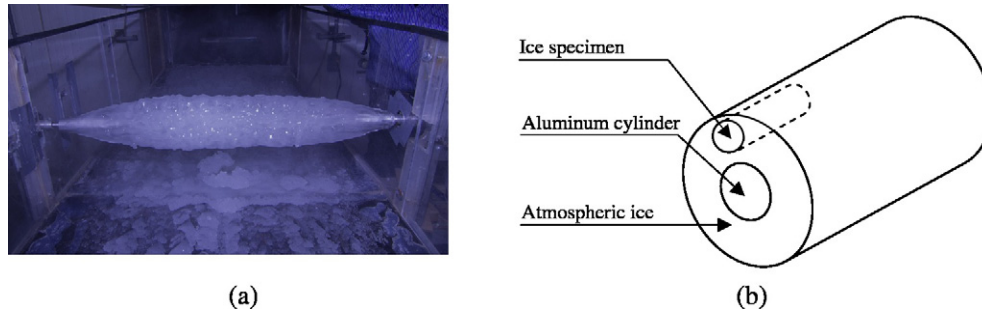


Fig. 1. Accumulated atmospheric ice on the rotating cylinder and sample cut (Farid et al., 2016).

Table 1

Ice density for different temperatures.

Temperature	− 15 °C	− 10 °C	− 5 °C
Density (g/cm ³)	0.79	0.81	0.89

and liquid water content (LWC) was chosen to be 2.5 g/m³. For each accumulation temperature, ice density was measured, as shown in Table 1. After the desired thickness of ice was obtained (>70 mm), cylindrical specimens were cut and machined. The specimens were 125-mm long cylinders of 50-mm diameter, their axial axis was parallel to the accumulation cylinder axis, as shown in Fig. 1(b). Cutting prismatic blocks from the rotating cylinder using a saw generates micro cracks, and therefore local stress concentration at the edges of the blocks, this was avoided using a warm cutting blade. Moreover, a special laboratory designed tool with flat edge was used for machining the cylindrical specimens, and the rotating speed during machining was kept slow enough to avoid any micro cracking. After the machining, the specimens were stored in the cold room at the same temperature during enough time to let them relax any residual stress. All the samples were tested at the same temperature at which ice had been accumulated.

When considering a three-dimensional stress state in a material, it is more convenient to distinguish three mutually perpendicular directions for which shear stresses disappear (Jaeger et al., 2009). These three directions also define the main normal stresses σ_1 , σ_2 and σ_3 . The convention adopted in this study is that $\sigma_1 \geq \sigma_2 \geq \sigma_3$, and that the compressive stresses are considered positive. The applied stress field to an atmospheric ice sample in a triaxial compression test is presented in Fig. 2. The confining stress, σ_{conf} , is applied by imposing a pressure to the fluid surrounding the sample; it is also called the principal minor stress

σ_3 . The differential stress ($\Delta\sigma$) is obtained by applying an axial displacement to the sample, this stress acts together with the confining stress in the axial direction. Combined, these two stresses are equal to the axial stress σ_a , also called major principal stress σ_1 .

Each sample was coated with a latex jacket, in order to isolate the ice and prevent it to come into direct contact with the confining fluid (oil). The sample then was mounted against the pusher piston and the alignment seat through two seals, as shown in Fig. 3. The purpose of this operation is to ensure the alignment of the samples without introducing any residual stresses.

The sample is introduced into the chamber without the presence of compressive fluid. Once the entire sample with piston is aligned and well concealed, the hydraulic pressure is gradually increased to reach the desired value. A relaxation time is needed to reach a pressure equilibrium before the beginning of the triaxial test.

All triaxial tests were performed with an MTS load frame equipped with a 250 kN load cell. The test system was located in a cold room with controlled temperature, ranging from 0 to −40 °C (± 1 °C). The confinement cell was equipped with a manometer to insure hydrostatic pressure stability. As the confinement cell was not equipped with any electrical port or sensor, the specimens could not be monitored while been pressurized. Therefore, the direct strain within ice could not be measured, hence it has been substituted by the normalized displacement, which corresponds to the total displacement, D ($D = d_{ice} + d_{actuator}$) divided by specimen length, L, and the nominal strain rate for a given test was determined from the crosshead speed divided by the specimens' length. Fig. 4 illustrates the different components of the triaxial test system. The confinement cell was supplied with hydraulic pressure through a pressure supply unit, having a maximum capacity of 20 MPa. The external load cell allowed a separate control of the hydrostatic pressure during the tests.

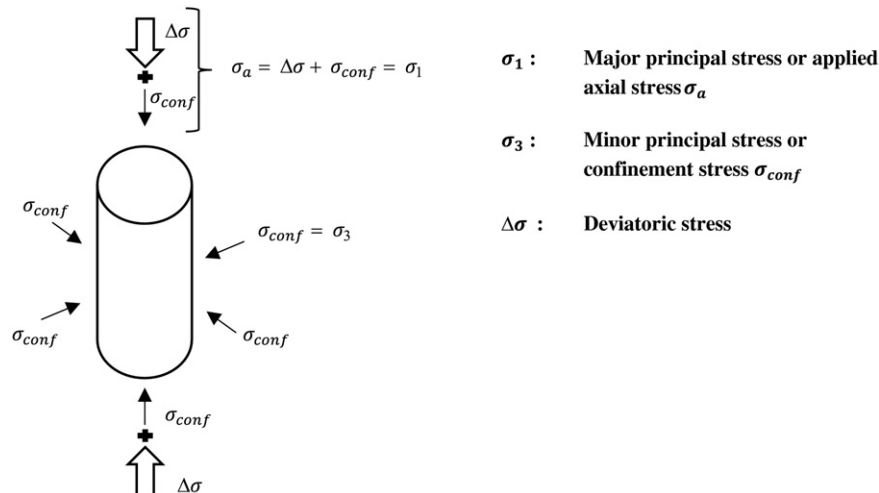


Fig. 2. Triaxial stress state.

Download English Version:

<https://daneshyari.com/en/article/5779410>

Download Persian Version:

<https://daneshyari.com/article/5779410>

[Daneshyari.com](https://daneshyari.com)